Available online at www.sciencedirect.com
ScienceDirect
International Journal of Impact Engineering 34 (2007) 1286–1305
INTERNATIONAL JOURNAL OF IMPACT ENGINEERING
www.elsevier.com/locate/ijimpeng

Computational analysis of impact of a bullet against the multilayer fabrics in LS-DYNA

Rimantas Barauskas[a,*], Aušra Abraitienė[b]

[a]*Department of System Analysis, Kaunas University of Technology, Studentų 50, 51368 Kaunas, Lithuania*
[b]*Lithuanian Textiles Institute, Demokratų 53, LT-3714 Kaunas, Lithuania*

Received 20 January 2005; received in revised form 19 December 2005; accepted 16 June 2006
Available online 22 August 2006

Abstract

A finite element model of the ballistic test against the multi-layer paraaramid textiles package structure has been developed in LS-DYNA. The bullet has been considered as a deformable body in contact with the fabric package represented by an interwoven yarn structure. The simplification of the model has been achieved by means of the "mezzo-mechanical" approach by avoiding the direct modeling of filaments comprising the yarns. Instead, yarns have been modeled by using thin shell elements the thickness of which represents the real thickness of yarns as it can be measured in the weave. The zones of the fabric remote from the point of impact have been presented as a roughly meshed uniform orthotropic thin shell model. The junction between the two types of zones of the fabric has been performed by means of the tie constraint and by proper adjustment of material parameters ensuring the same speeds of wave propagation in the interwoven yarn structure and in the uniform shell. Physical and numerical experiments have been performed in order to identify the material model parameters and to validate the model.

Keywords: High-velocity impact; Multi-layer fabric; Finite elements; Mezzo-mechanical model; LS-DYNA

1. Introduction

The clothes ensuring the ballistic protection have to be designed in a way that their ballistic strength exceeds many times the rates intended in regulating standards and ensures the necessary protection level. For the estimation of the ballistic safety the worldwide spread USA standard NIJ 01.01.04 is employed. During the experiments the interception of bullets by multi-layer fabric packages (MLFP) have been registered for a wide spectra of values of the kinetic energy of bullets depending upon mass and velocity of a bullet, as well as, the type of a weapon. The results obtained during the investigation of multi-layer textile packages designated for bullet-resistant vests at the Lithuanian textile institute imply that the protection level is defined by the following basic factors [1]:

– Yarns: the number of filaments comprising a yarn, linear density, maximum force and elongation, stiffness modulus.

*Corresponding author.
E-mail address: rimantas.barauskas@ktu.lt (R. Barauskas).

0734-743X/$ - see front matter
doi:10.1016/j.ijimpeng.2006.06.002

– Fabrics: weave type, surface density, isotropy of the weave, tensile characteristics, trimming.
– Fabric package: number of layers and their interconnection technique.

The rapid rise and variety of new textile materials on the market, [2], promotes the further theoretical and experimental investigations of fabric packages by establishing their properties and regularities. The design of MLFP can be significantly facilitated by means of deeper understanding of the behavior of a single or several fabric layers during their interaction with bullets. The results obtained from computer simulations could expedite the selection of a structure of a package designated for ballistic tests and simultaneously decrease the expenditures needed for optimization of packages made of fabrics of different surface density and different constitution.

The experimental investigations of ballistic interaction are complicated because of very large velocities, deformations and failure of interacting structures. Conventional experiments mostly provide integral characteristics of the processes such as the pre- and post-impact velocities, extent of final failure of the projectile and the target, etc. The main shortage of such kind of results is their inability to provide the insight into the interaction processes and to clarify transient dynamic processes and failure mechanisms taking place at the contact zone. During the last decade numerous researches have been carried out on the ballistic impact on high strength fabric structures [3–6].

The high velocity contact interaction problems are among the most complicated in computational mechanics. The failure processes that follow the interaction are initiated in micro-volumes considerably smaller than the measurements of the interacting bodies. It is practically impossible to model the behavior of the material in the micro-volume as the number of degrees of freedom of such a model would be too large and unrealistic for available computer resources at the time being and probably in the nearest future as well. In [7], real and numerical shooting-through experiments are presented for the Nextel textiles and the Kevlar-epoxy shield. The micro- and mezzo-mechanical models have been used to simulate the behavior of small specimens in AUTODYN. By comparison of the numerical results against the experimental data, the material model characteristics have been determined in terms of the stiffness coefficients and the equation of state establishing the relationship between the pressure and the volume change. On this base real structures have been presented by using macro-mechanical models in which the multilayer has been presented as porous continuum. This enabled to disregard the real geometry of the weave and to present the averaged strength parameters of the textiles. The resulting model was axially symmetric, had a reasonable dimension and the obtained results were satisfactorily close to experimental ones. The problems including flexible textile structures such as clothes are very difficult to represent by equivalent solid models as after the failure of yarns the geometry of the model becomes very complex. In [8] and [12], a computational model in LS-DYNA has been presented. It enabled to consider the geometry of the weave by using shell elements. Numerous approaches have been presented where yarns of a weave were modeled by using 3D solid elements [6,9,10].

The aim of this work is to develop a computational model of interaction of a deformable projectile (bullet) against a MLFP enabling to simulate shooting experiments performed in order to test the ballistic strength of the textile body armor. For the sake of reduction of the dimensionality of the computational model the mezzo- and macro-mechanical approaches have been combined together. The mezzo-mechanical approach is employed in order to present multi-filament yarns by means of shell elements. In this way, the ballistic interaction zone is presented as a structure of interwoven yarns. The macro-mechanical approach is being used for modeling of the surrounding of the woven patch of a fabric as a uniform membrane. Comparisons with the experimental results have been carried out in order to determine the dynamic parameters of the material behavior and to validate the model.

2. The architecture of the model

2.1. Bullet

The bullets used during the ballistic strength evaluation tests can be very different subject to the required safety level. In this study, we employ the finite element model of the 6 mm lead bullet BALLE 22 presented in Fig. 1. The finite element mesh of the model has been obtained by using TrueGrid software.

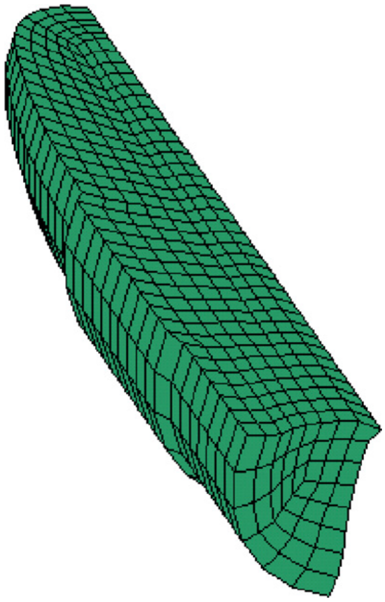

Fig. 1. Quarter-symmetry finite element model of BALLE22 lead bullet obtained by using the TrueGrid software.

2.2. Woven fabric patch

Each fabric layer is made of yarns of certain linear density woven together. Each yarn consists of filaments the number of which can vary from several hundred to several thousand. The model of a fabric at the level of filaments is unrealistic because of limited computer resource, so we develop a mezzo-mechanical model in which a yarn has been considered as primary component comprising a fabric. The properties of an individual yarn are defined empirically by making several assumptions.

It is commonly accepted that the cross-section of a free yarn not interwoven into a textiles is close to a circle made of cross-sections of a certain number of individual filaments, Fig. 2a. In a fabric, the yarns are being compressed because of forces acting in overlapping areas. As a result, the geometry of the cross-section of each yarn is being changed depending upon the constitution of the yarn, its density, its type and technological parameters of the weave. After examination of the cross-section of the yarn extracted from the fabrics we assume it to be close to the combination of two circular segments, Fig. 2b. The dimensions of the circular segments comprising the cross-section are calculated based upon the given characteristics of the fabric. E.g., the height and length of the yarns in the paraaramid Twaron textiles CT709 are $b = 0.952\,\mathrm{mm}$ and $h = 0.15\,\mathrm{mm}$, the density of the material is $1440\,\mathrm{kg/m^3}$, and the stiffness modulus in extension is 90 GPa.

The cross-section of a yarn interwoven into a fabric has been modeled as shown in Fig. 2c. As its height is much smaller than the width, we used four shell elements the thicknesses of which were selected in order to fit two circular segments form. The bending stiffness of a yarn we assumed to be negligible. In order to eliminate the bending stiffness in LS-DYNA the Hughes-Liu shell element with single integration point through the thickness of the element has been used. The technique of obtaining the model of a woven yarn patch in more detail has been described in our recent work [8]. By using this technique, the weave is obtained by solving the contact interaction equilibrium problem and is able to present the *warp* and *weft* yarns in the weave. The Ox directed yarns (the warp) are elastically deformed by moving their nodes in the direction Oz perpendicular to the plane of the layer in order to situate the Oy directed yarns (the weft) in-between the warps. After activation of the contact search algorithm the yarns of the model come to an elastic equilibrium. As a result, a woven structure is obtained in a similar way as a real fabric is produced. After equilibrium is obtained, the elastic stresses and strains are being fully or partially removed in order to imitate the relaxation of stresses in multi-filament yarns. Moreover, we may control the amount of the residual stress. In this way, we may create a desired value of the warp tension that is an important characteristic of a weave.

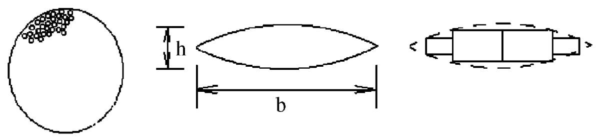

Fig. 2. (a) Circular cross-section of a free yarn; (b) cross-section of an interwoven yarn approximated by two circular segments; (c) cross-sections of an in-woven yarn approximated by rectangular cross-sections of four shell elements.

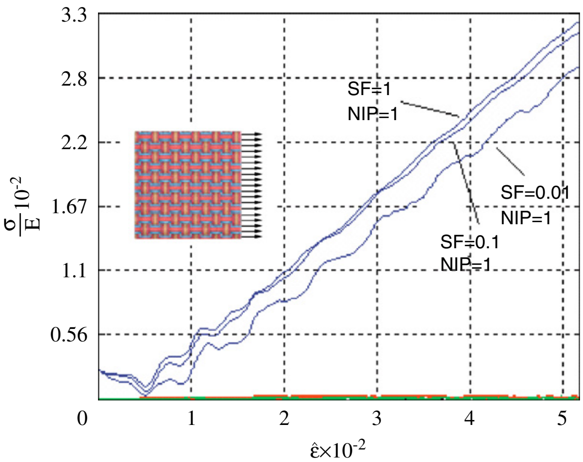

Fig. 3. The relationships of the longitudinal strain σ/E in a yarn against the relative elongation $\hat{\varepsilon}$ of the textiles in the warp direction at different values of the slave contact stiffness scale multiplier SFS.

The obtained model of a fabric is able to present the mobility of one yarn system with respect to the other and small shear stiffness in its plane. The elongation of a fabric in tension consists of two components: the elongation caused by de-crimping of yarns and their tensile elongation. As the strain–stress relationship of the paararamid material remains practically linear up to the tensile failure limit, the longitudinal strain can be measured as σ/E, where σ—traction applied to the yarn, E—stiffness modulus. The relation of ratio σ/E against the relative elongation $\hat{\varepsilon}$ of the fabric is presented in Fig. 3. The results of tension experiments upon fabric specimens demonstrate that the failure takes place at 4–5% elongation of the fabric, whereas a straight paraaramid yarn fails at 3% elongation.

In reality, the de-crimping of yarns caused by the extension of the fabric is accompanied by the deformation of the cross-sections of the yarns. It is necessary to note that the model of a yarn composed of shell elements is not able to present any further change of the thickness of a yarn caused by transverse forces perpendicular to the shell element. Consequently, the presented woven fabric model inherently has an enlarged tensile stiffness caused by lesser de-crimping of yarns as it is in reality. Nevertheless, an imitation of the through-thickness deformation in the model still may be achieved by selecting an appropriate value of the penalty stiffness coefficient that determines the magnitude of the repelling force when two surfaces are intending to penetrate into each other in the condition of a mechanical contact. Lesser values of the penalty coefficient allow greater penetration during the transverse yarn-to-yarn contact. The depth of penetration of yarn surfaces into each other make influence on the extent of their de-crimping, or may be interpreted as the change of thickness of a yarn. In LS-DYNA, the penalty coefficient can be adjusted to a necessary value by selecting a proper value of its scale multiplier referred to as SFS in LS-DYNA Keyword manual. By selecting value of SFS in the range 0.01–1 for different kinds of yarns and different types of a weave we may control the shape of the static deformation curve and make it close to the one obtained experimentally.

2.3. Single layer of a fabric

The zone of a fabric proximately taking place in the contact interaction for a 9 mm bullet comprises only about 20–60 mm in diameter. However, in order to represent properly the dynamics of the interaction process much larger pieces of a fabric should be modeled. The duration of the interaction process is generally conceived as the time from the beginning of the impact until it reaches zero velocity embedded into the multilayer or until the time moment when the fabric is completely perforated. During this time, the longitudinal deformation wave propagating from the point of impact travels much larger distances, so the linear dimension of the fabric being modeled should be at least ~200–400 mm. Unfortunately, the weave step being about 1 mm, such ‘‘fully woven’’ models are prohibitive because of their huge dimensionality. As an example, the dimension of 12 fabric layers quarter-symmetry model may reach $\sim 10^8$ nodes. In order to obtain smaller models the macro-mechanical approach is being used. The zones of the fabric remote from the interaction zone are modeled by means of orthotropic shell (membrane) elements that can be much bigger than the elements presenting the mesh of the yarns.

Sudden transitions in mesh density of finite element models are implemented by using tied interfaces. This feature may decrease the effort to generate the meshes since it reduces the need to match nodes across interfaces of merged parts [10]. In LS-DYNA, the finely and roughly meshed zones are connected by using the *CONSTRAINED_TIE-BREAK constraint, Fig. 4. We prohibit the failure of the constraint by using very large failure strain values and no-failure material model for the yarns neighboring to the membrane model nodes. The reason for such numerical ‘‘failure prevention’’ measure is that the algorithm of implementation of tied interface constraints in LS-DYNA tends to overestimate the strain values in local zones of refined mesh adjacent to the roughly meshed membrane domain. Sometimes a situation may occur when the locally overestimated strain value may cause a failure of a yarn where it appears to be not realistic physically. Such fictitious strain effects may cause to some extent numerical distortions or reflections of waves propagating across the tied interface.

A uniform membrane-type surrounding of the woven patch cannot be expected to present an identical dynamic behavior as the woven yarn structure. However, satisfactory approximation is possible provided that the appropriate selection of geometrical and physical properties of the membrane zone is made. Two models of the fabric layer with different dimensions of the woven patch are built, Fig. 4. The model containing a larger patch has been considered as a reference model (in our study it contained 120 × 120 yarns), and the smaller one was 20 × 20 yarns; we take it at least twice greater than the diameter of the zone at which the failure of yarns may take place. By taking into account the quarter-symmetry of the model we have to build 10 × 10 and

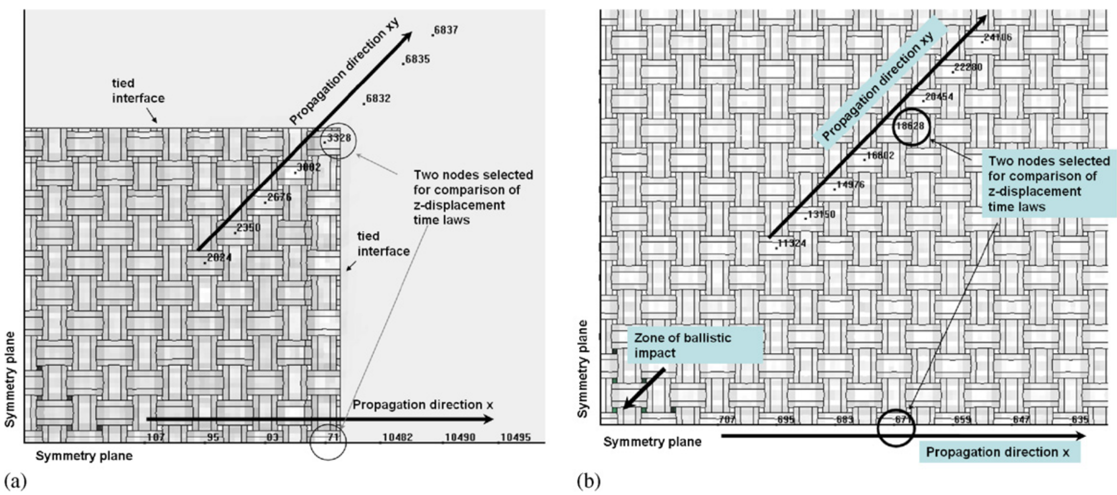

Fig. 4. Fragments of woven fabric quarter symmetry models with indicated wave propagation directions and numbers of nodes for comparison of dynamic properties: (a) woven patch 10 × 10 yarns; (b) fragment of the woven patch 60 × 60 yarns (reference model).

60×60 yarn woven patch models correspondingly. The size of membrane-type surrounding of the patches is much larger than the woven patches, however, the total linear dimension of each model is the same.

The membrane is presented by 1-integration point shell elements exhibiting no bending stiffness. The membrane thickness may be assumed as known, however, the values of mass density ρ, Young's modulus E and shear modulus G of the orthotropic material have to selected in order to obtain the dynamic response of both models as close as possible to each other. In LS-DYNA, the orthotropic material can be defined as *MAT_ORTHOTROPIC_ELASTIC or *MAT_FABRIC. The best results can be expected if the selection of parameters is accomplished for the dynamic behavior close to the specific analysis situation. In this work, the numerical tests are performed for the 270–300 m/s impact and perforation of the fabric by the lead bullet.

The overall approach is similar to the convergence investigation of models with different levels of refinement. The "exact" numerical solution may be regarded as known as we are able to make a stand-alone numerical experiment by employing the fully woven model. Further a series of models with different sizes of the woven patch are investigated and the physical constants of the surrounding orthotropic membrane established in order to ensure a convergent behavior in the sense that the solutions obtained by using every model are close to the exact one. This could be referred to as the verification of the model of a fabric layer arranged by employing a combination of mezzo- and macro-mechanical approaches. We limited the analysis to comparison of the dynamic behavior of two models only because of limited amounts of the computational resource.

In our investigation the comparison of the dynamic behavior of the two models has been performed in terms of:

- variation of the propagation speed of the longitudinal and transverse in the vicinity of the tied interface of the model. Two wave propagation directions are investigated: direction x along axis Ox and direction xy along the line $y = x$, Fig. 4;
- time laws of z displacement of two selected nodes;
- time instant of initiation of failure of the fabric;
- time instant of full perforation of the fabric.

In order to estimate the wave propagation speed as the wave propagates in between two nodes of the structure we fix time moments t_1, t_2 when the displacements of the nodes reach a pre-selected level, see Figs. 5a and b. For instance, the average speed of the wave propagating along direction x may be estimated as $v = \Delta x/(t_2 - t_1)$, where $\Delta x = x_2 - x_1$—distance between the nodes. The longitudinal and transverse wave propagation speed estimated along direction x is presented in Fig. 5c,d. The discontinuities in the wave propagation speed relationships are eliminated at each nodal point by taking the average of the propagation speeds in two neighboring inter-nodal segments of the wave propagation line. The curves representing the variation of longitudinal and transverse wave propagation speeds estimated along the diagonal direction xy are presented in Fig. 6.

The results presented in Figs. 5 and 6 are obtained by using one of "successful" sets of membrane material constants as

$$\frac{\text{Surface density of the membrane}}{\text{Surface density of the woven patch}} = 0.8;$$
$$\frac{\text{Young's modulus of the membrane}}{\text{Young's modulus of the yarn}} = 0.3;$$
$$\frac{\text{Shear modulus of the membrane}}{\text{Young's modulus of the membrane}} = 0.0042.$$

Rather small value of Young's modulus of the equivalent membrane enables to present the de-crimping driven deformation of the fabric which can be expected to prevail in zones remote from the point of impact. Very small values of shear modulus are quite natural to expect because of small shear stiffness of a woven structure at small strains. However, the value of shear modulus had to be selected with care as it makes a

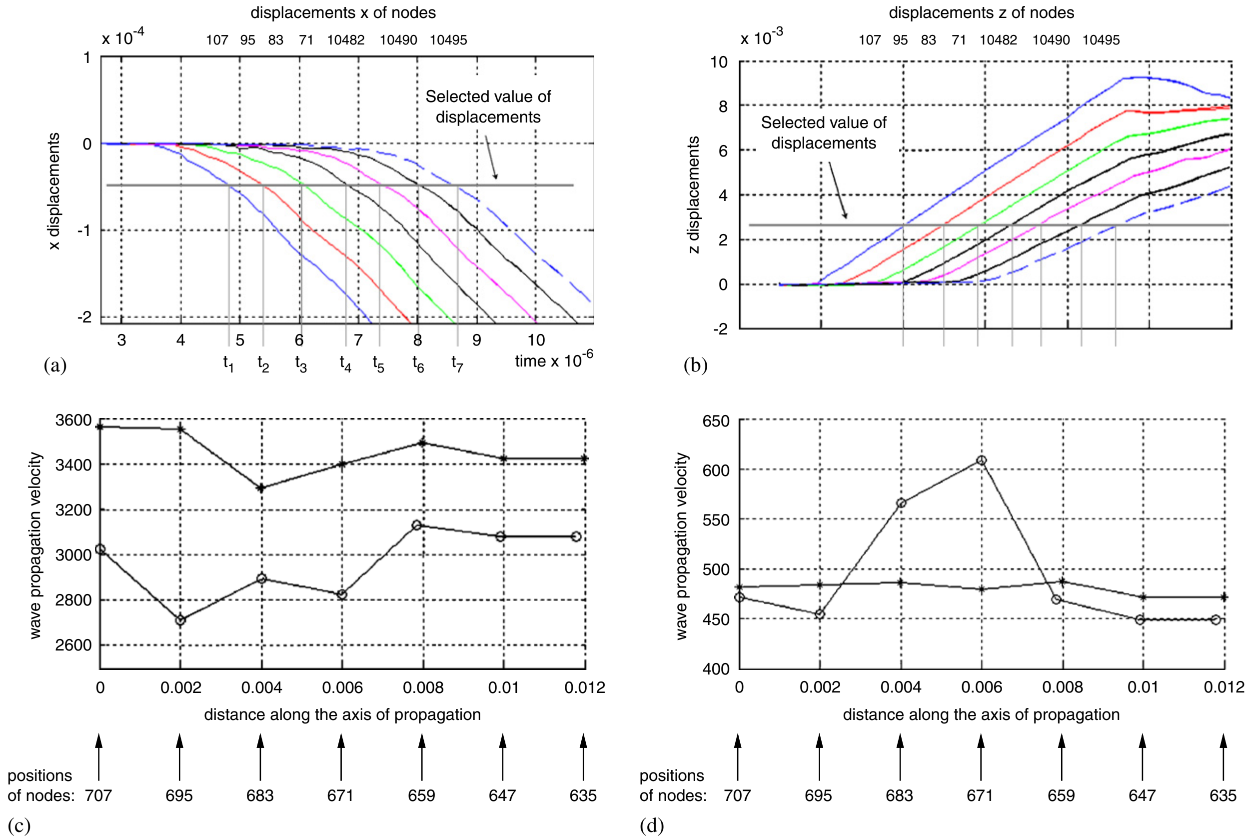

Fig. 5. (a,b) Time laws of longitudinal (a) and transverse (b) displacements of nodes and determining impact wave propagation speeds along direction x in the vicinity of the tied interface; (c,d) estimated propagation speeds of longitudinal (c) and transverse (d) waves along direction x in the vicinity of the tied interface: (-o-) obtained by using model (Fig. 2a); (-∗-) obtained by using the reference model (Fig. 2b).

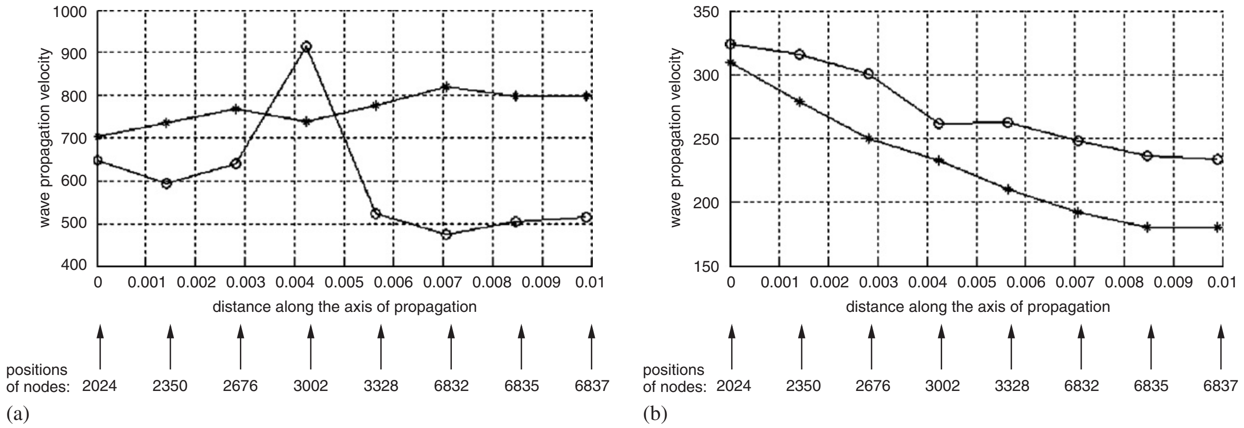

Fig. 6. Estimated propagation speeds of longitudinal (a) and transverse (b) waves along direction xy in the vicinity of the tied interface: (-o-) obtained by using model Fig. 2a; (-∗-) obtained by using the reference model Fig. 2b.

significant influence basically upon the shape of the front of the transverse wave, as well as, upon its amplitude.

It should be noticed that the wave propagation speed relationships of the reference model and 10×10 woven patch model have significant (up to $\sim$20%) differences. In order to quantify the differences we introduce the relative cumulative wave propagation speed error (CWPE) as

$$\mathrm{err} = \frac{\int_0^L |v - v_{\mathrm{ref}}|\,\mathrm{d}x}{\int_0^L |v|\,\mathrm{d}x},$$

where v, v_{ref}—wave propagation speeds estimated by using both models, L—length of the selected wave propagation path.

The CWPE values for the case presented in Figs. 5 and 6 are as follows:

- In propagation direction x, displacement direction x: $\mathrm{err}_x^x = 0.19$.
- In propagation direction x, displacement direction z: $\mathrm{err}_z^x = 0.068$.
- In propagation direction xy, displacement direction x: $\mathrm{err}_x^{xy} = 0.35$.
- In propagation direction xy, displacement direction z: $\mathrm{err}_z^{xy} = 0.16$.

CWPE values in the diagonal direction xy are about twice larger than in direction x. Anyway, the change of the membrane material parameters causes the changes in CWPE as well. CWPE relationships corresponding to different wave propagation directions may exhibit different tendencies to increase or decrease as a consequence of the same change of the membrane material parameters. Though the obtained CWPE values are not very small even in engineering sense, the resultant displacements and wave fronts obtained by using 10×10 model are close to the results obtained by using the reference model as can be observed from the results presented in Fig. 7.

Our investigation demonstrated that it is hardly possible to select the membrane material properties ensuring very good approximation to the woven structure behavior in all stages and aspects of its motion. For example, the model that properly represents the process of failure of the fabric may produce certain displacement errors in representing its motion after the perforation, see Fig. 7g, h. On the contrary, a model adequately representing the after-perforation motion of the fabric may produce inaccuracies in estimating the time instant of the initiation of the failure. In the ballistic interaction problem, the proper representation of the time moment of beginning of failure of the fabric is of primary importance, therefore by adjusting the membrane layer parameters it has been achieved that the failure begins in both models at the same time instant.

Better results can be expected by using non-linear material models of the membrane, however, we did not perform such investigations in this study. On the other hand, non-linear material models often suffer from the lack of stability when the tangent of the stress-strain curve increases with increasing strain (e.g. *MAT_NON_LINEAR_OTHOTROPIC of LS-DYNA).

2.4. Contact interaction model

The developed model of a single fabric layer has been used further for the analysis of the ballistic impact of a bullet on a MLFP. The view of the contact model symmetrical with respect to xOz and yOz planes is displayed in Fig. 8. The MFLP model is obtained by making copies of the obtained model of a single fabric layer. The number of copies is equal to the number of layers required in MFLP. The copies are appropriately positioned in the direction of Oz axis. Each copy acquires individual numbers of elements and nodes. A space between adjacent layers of MFLP cannot be strictly defined or determined in the formulation of the problem. In reality, we have to deal with a package of free fabrics interlinked by seaming them together as it is common practice in constructions of ballistic protection clothes. The distance between adjacent seams is usually many times greater than the thickness of a yarn, therefore, spaces between adjacent layers may be variant throughout the same package. Obviously, at this point a simplification is necessary, so we positioned fabric layers one from another with spaces comprising ~30% of the thickness of a single layer.

In order to make copies of a single fabric layer in LS-DYNA we have to take into account that the model is obtained as a result of the contact interaction problem solution [8]. Therefore, all copies of the single layer have to contain all the information about final geometry of crimped yarns, their stresses and strains, as well as, about contact interaction conditions between yarns. In LS-DYNA such information is retained by using *INTERFACE_SPRINGBACK keyword; the resulting file contains all the information necessary for

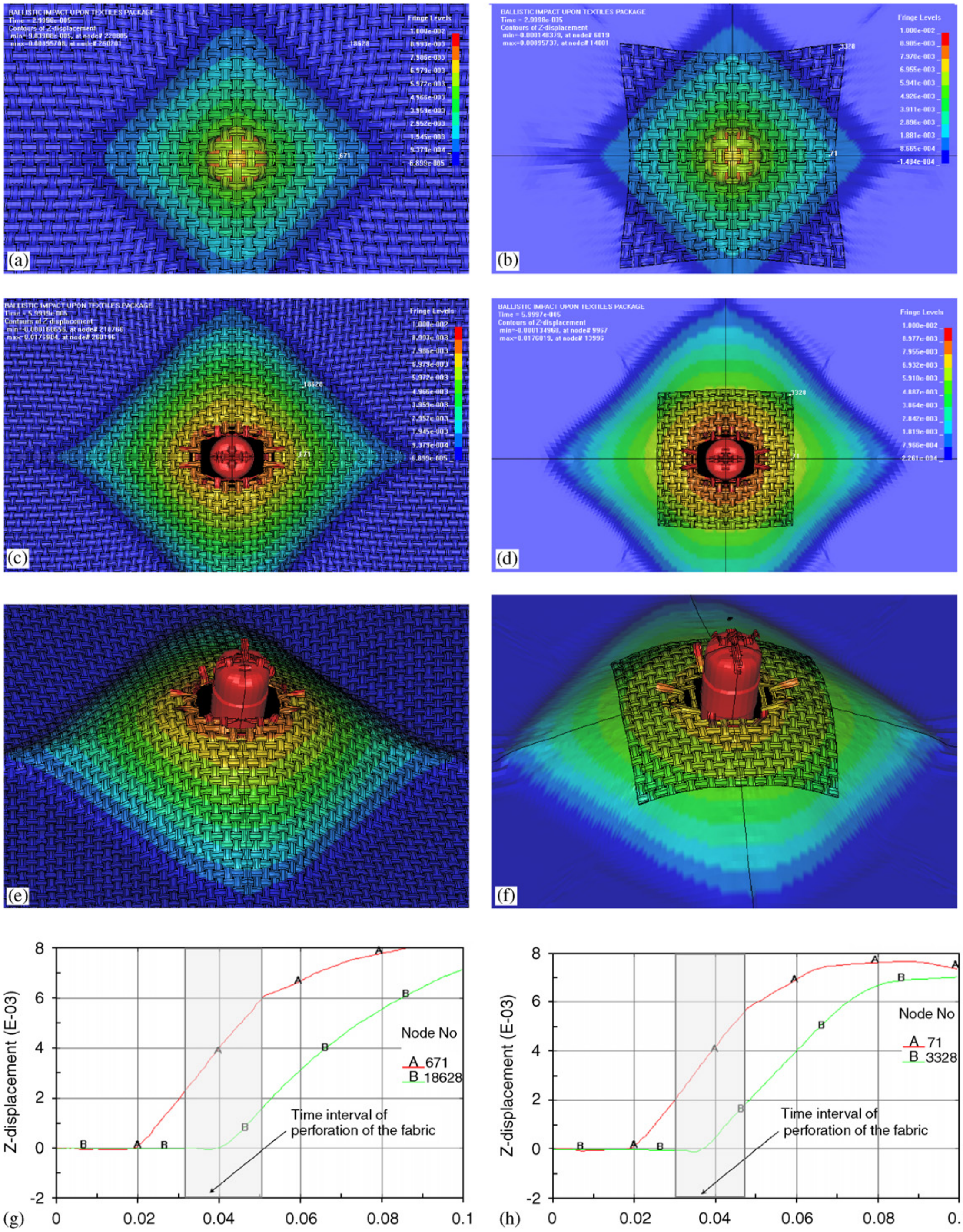

Fig. 7. The shape of the transversal wave front and z-displacement contour plot obtained by using reference model (a,c,e) and 10×10 combined model (b,d,f): (a,b) at time instant 3×10^{-5} s (beginning of the failure); (c,d) at time instant 6×10^{-5} s; (e,f) at time instant 6×10^{-5} s (axonometric view); (g,h) z-displacement time laws of two selected nodes as indicated in Fig. 4.

re-building the single layer woven fabric model in a new run of the program. The necessary transformations, such as re-numbering of items, changing spatial positions of parts, etc., are performed by writing a case-oriented software for processing the corresponding data files.

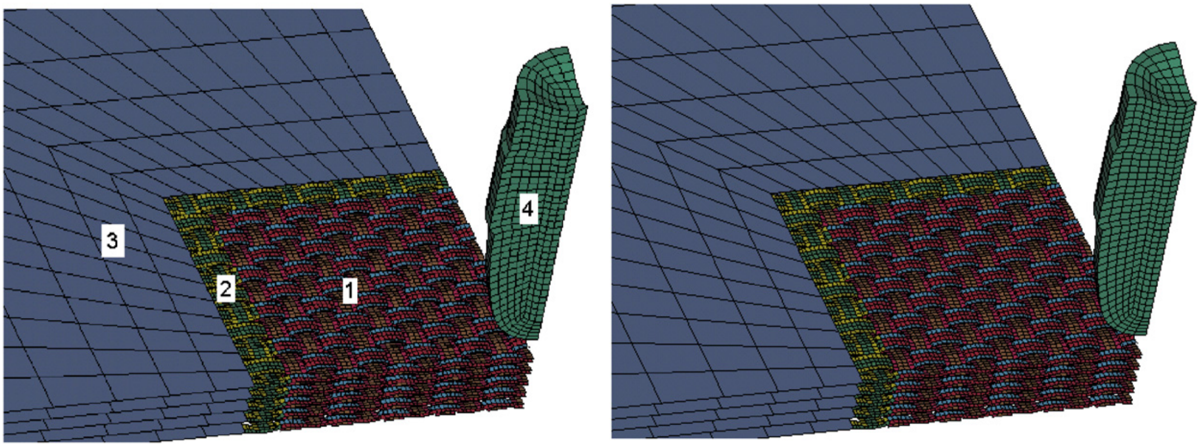

Fig. 8. Woven structure model tied to the membrane model: (1) woven structure, material model with failure; (2) woven structure, no failure; (3) membrane zone; (4) bullet.

3. Material models

The materials taking place in the contact interaction of a bullet against the multilayer fabric are the lead and the paraaramid. The lead is an elastic-plastic material, and paraaramid is perfectly elastic up to its failure limit.

Only two material models: *MAT_ELASTIC and *MAT_PLASTIC_KINEMATIC are used in this analysis. *MAT_ELASTIC we use for paraarmid in the initial stage of formation of the woven patch, see Section 2.2. In subsequent stages, this material is changed to *MAT_PLASTIC_KINEMATIC by assuming the yield strain equal to the failure strain. *MAT_ELASTIC during all the calculation is maintained only for yarn elements neighboring to membrane region as motivated in Section 2.3.

For the lead material *MAT_PLASTIC_KINEMATIC is used with elasticity modulus, Poisson's ratio and density considered as prescribed. At ~300 m/s impact velocity, the problem is classified as high velocity contact–impact interaction problem where the yield stress value is assumed to be dependent upon the strain rate in accordance with the Cowper–Symonds material model [11]:

$$\sigma_Y = \sigma_{Y0}\left[1 + \left(\frac{\dot{\varepsilon}}{C}\right)^{1/p}\right], \tag{1}$$

where σ_Y, σ_{Y0}—yield stress limits of the material defined with and without the influence of strain rate $\dot{\varepsilon}$; C and p—constants.

Constants C, p and the tangent modulus of the lead, as well as, failure strain of paraaramid at high strain rates are finally specified on the base of comparison of the results of properly planned numerical and physical experiments as discussed further in the text.

The dry contact friction law between each pair of contacting fabric layers and between yarns interacting in the weave is assumed. The value of the friction coefficient exhibits a marked influence upon the interaction behavior. The procedure of determining the friction coefficient values and argumentation on this question is presented is Section 4.3.

During the contact interaction process the elements of the fabric, as well as, of the bullet are highly deformed and require to decrease the time integration step that in explicit integration techniques cannot be greater than the least time duration during which the elastic longitudinal wave passes the smallest element of the structure. As the simulation goes on, the time step tends to become shorter and solution may never end. We use the following methods of time step size control implemented in LS-DYNA:

- Artificial increase of the mass of shell elements that are causing the decrease of the time step under the prescribed limit.
- Deletion of solid elements that are causing the decrease of the time step under the prescribed limit.

Time step size control measures can be regarded as common practice in explicit dynamics calculations where very large strains are expected. They can be interpreted as a ‘‘safety catch’’ activated in order to cope with the elements that loose their physical meaning because of excessive straining. In most cases overstrained elements to which the mass scaling has to be applied are very small in all dimensions because of compression, consequently, the added amount of the mass is negligible. The highly strained elements that are not very small usually undergo extension in at least one direction. In this way they exceed their failure strain value and are removed from the structure earlier than they become overstrained.

4. Model validation and results

4.1. General approach

The adequacy of the obtained results to reality is a highly important question in any simulation. In the case of the system under consideration, two main sources of possible inadequacy can be mentioned:

– The ‘‘mezzo-mechanical’’ concept of the model, where the multi-filament structure of a thread is highly simplified.
– The use of the “macro-mechanical” concept for presenting the “infinite” fabric environment of the woven patch.
– Unknown dynamic values of the dynamic parameters of a material. At 300 m/s impact velocity the static relationship of yield stress against the plastic strain does not adequately describe the real physical phenomena. This circumstance is important for both materials participating in the impact interaction—lead and brass.

Though we used simplest model (1) to modify the yield stress value by taking into account the strain rate, physical and numerical experiments are necessary in order to obtain physically adequate values C and p, as well as, a proper hardening model which may appear as crucial for obtaining adequate results. We assume the elasticity and shear modules, the ‘‘static’’ yield stress and mass density of each material as known. The tangent modulus, values C and p in relation (1) and the kind of hardening hypothesis (kinematical, isotropic or the combination of the two) can be assumed as parameters the values of which need to be determined in order to achieve the adequacy of simulation results to reality. A series of case oriented experiments has been performed in order to determine the model parameter values step by step. The basic experiments we made in order to validate the model were as follows:

– shooting a lead bullet against the 10 mm thickness lead plate thus considering a problem with only one unknown material—the lead;
– shooting a lead bullet against a single fabric layer. The properties of the bullet model having been determined during the previous step, now again we had single unknown material—the paraaramid weave, friction coefficients of which could be determined;
– shooting a lead bullet against a MLFP. The experiment provided the data enabling to qualify the correction of the paraaramid failure strain value for the range of strain rates corresponding to ~300 m/s impact.

4.2. Determining the lead material parameters

As an experiment for validation of lead material parameters we used numerical and physical experiments of shooting the lead bullet into 10 mm thickness lead plate in order to have only one unknown material. The data obtained from the physical experiment were the measured linear momentum supplied by the bullet to the plate and the deformed shape of the bullet imbedded into the target.

The values of elasticity modulus E, Poisson’s ratio PR and mass density RO were considered as given in Table 2 (here we employ notation used in LSDYNA). The coefficients C (SRC) and p (SRP) of relationship (1), as well as, tangent modulus ETAN and parameter BETA were selected in order to obtain the simulation results close to experimental ones. From static tests the value of ETAN is known as 5.43E + 07, however, our analysis demonstrated that the diminished value 1.5E + 07 provides the adequate behavior of the model. The explanation for this may be that the contacting bodies are hot (the bullet is hot because of heat exchange in the rifle, and also the contact interaction releases considerable amounts of heat). Parameter BETA < 1 determines the weight coefficient of kinematical hardening, and (1-BETA) gives the amount of the isotropic one. We chose the BETA value ensuring the hardening law closer to isotropic in order to get the results close to experimental. The choice of the type of hardening law may influence the results dramatically, Fig. 9. Fig. 9a presents the original shape of the bullet and Fig. 9b–d demonstrate and deformed shape of the bullet imbedded into the plate by using three different values of BETA. The situation in Fig. 9d with BETA = 0.2 is in the best coincidence with experimental dimensions measured according to the scheme presented in Fig. 10. The enlarged photo of a crater made by the lead bullet imbedded into a lead plate is presented in Fig. 11. Table 1 presents experimentally measured and numerically obtained values of geometric dimensions of the crater and of the bullet remains. The lead material parameters used in this calculation are presented in Table 2.

The presented values of material parameters were obtained by revealing material parameters responsible for this or that feature of the solution rather than by simply trying ‘‘mixes’’ of parameters. For example, the geometrical shape of the highly deformed bullet is mainly dependent upon coefficient BETA, Fig. 9. The effect of the BETA value could not be replaced by ‘‘mixing’’ values of other parameters. The depth of the crater was mainly dependent on the value of the tangent modulus and the scaling parameters of the yield stress SRC and SRP. We had many computed and experimentally obtained geometrical dimensions to be compared (Table 1), and only few material parameters to be qualified such as ETAN, BETA, SRC and SRP (Table 2). So we are inclined to state that the ‘‘accidental mix’’ of parameter values is not probable. On the other hand, the procedure of parameter value adjustment here is not ‘‘formalized’’, though actually it should be considered as a mathematical procedure of parameter identification. Naturally, to a certain extent the parameter value set can appear as ambiguous. For example, ambiguity is possible while selecting parameters SRC and SRP. Both

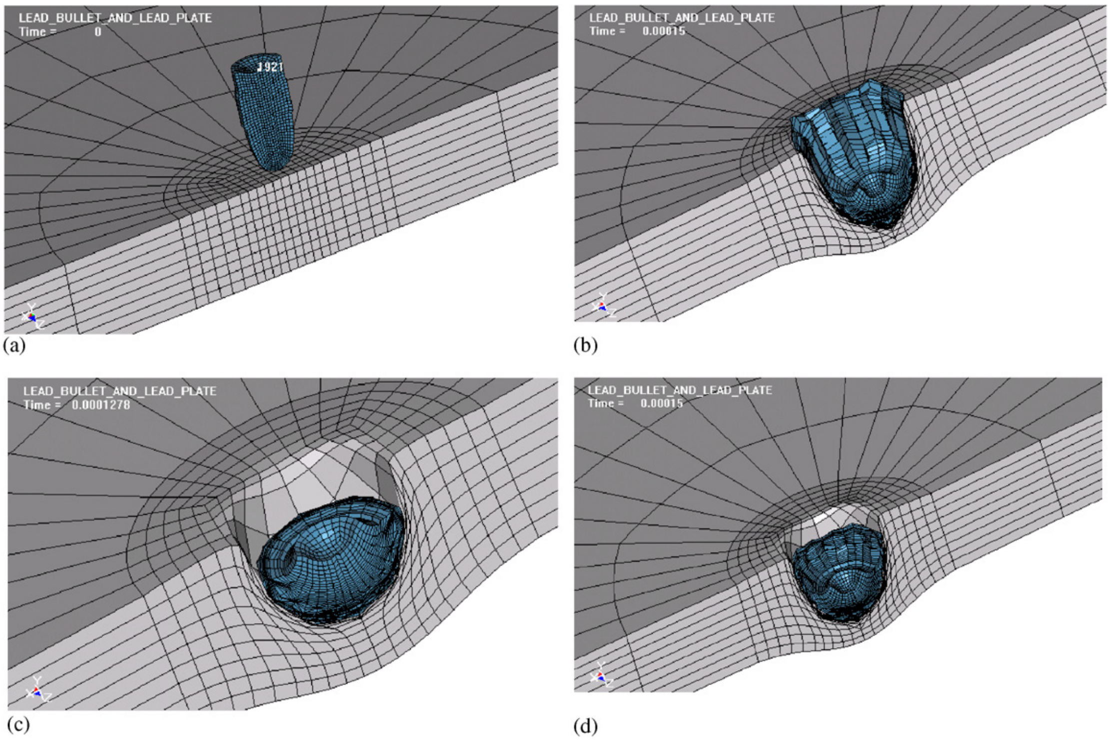

(a) (b) (c) (d)

Fig. 9. Impact of a lead bullet against a lead plate: (a) initial position, velocity 270 m/s; (b) final position (velocity 0) by using parameter BETA = 0; (c) final position (velocity 0) by using parameter BETA = 1; (d) final position (velocity 0) by using parameter BETA = 0.2, satisfactory coincidence with the experiment.

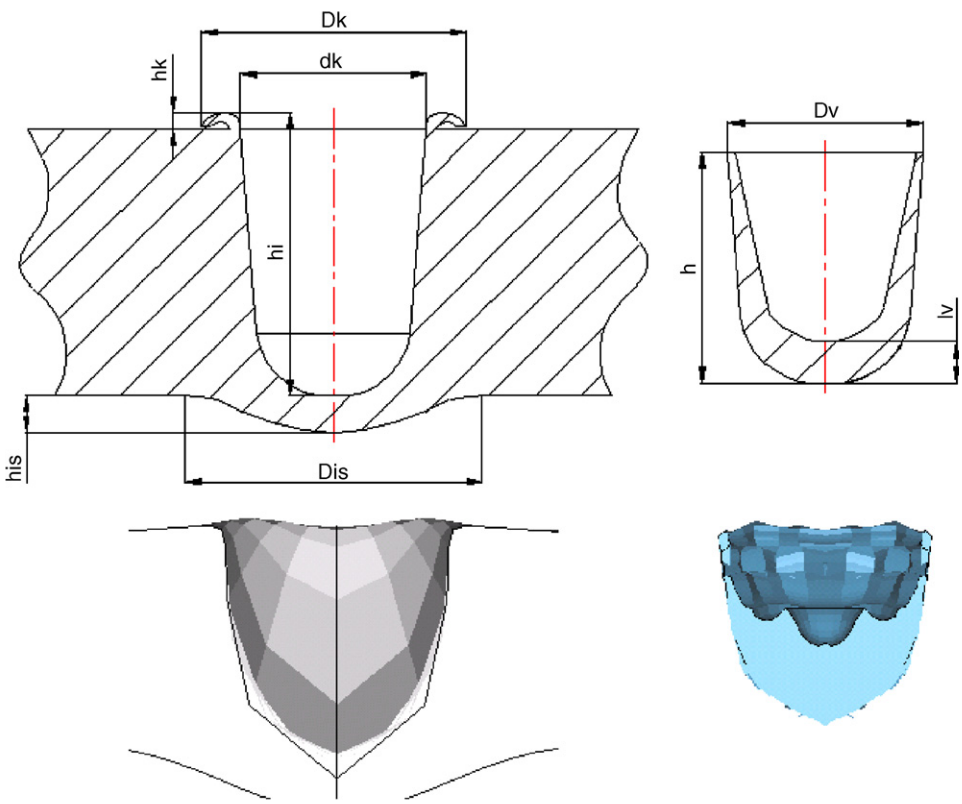

Fig. 10. Sketches (top) and simulated views (bottom) of the scheme of the experimentally measured dimensions of the crater made by the lead bullet in a lead plate (a) and of the remains of the bullet (b).

Fig. 11. Photo of a crater made by the lead bullet imbedded into a lead plate. Inside of the crater the remains of the bullet can be seen.

of them belong to Symonds–Couper yield limit scaling model and to some extent are able to compensate each other. Subtle experiments are necessary to determine the proportion between SRC and SRP precisely. It may be an object of another deeper study.

Table 1
Experimentally measured and numerically obtained values of geometric dimensions of the crater and of the bullet remains (see Fig. 8)

Dimension	D_k	d_k	h_k	h_i	D_{is}	h_{is}	m_l	D_v	h	l_v
Experimental (mm)	13.27	9.34	1.82	13.34	14.89	4.77	2.36	8.93	9.75	3.03
Simulated (mm)	–	11.00	–	11.30	19.00	3.20	2.23	10.20	9.40	3.80

Table 2
Parameters of lead material model used in LSDYNA (all units in SI)

Parameter	RO	*E*	PR	SIGY	ETAN	BETA	SRC	SRP
Value	11270	1.7E+10	0.4	8.00E+06	1.5E+07	0.1–0.2	600	3

Table 3
Parameters of paraaramid Twaron material model used in LSDYNA (all units in SI)

Parameter	RO	*E*	PR	SIGY	FStrain
Value	1400	9.0E+10	0.3	3.60E+09	0.04

4.3. Determining friction coefficients of the woven structure

As an experiment for validation of material parameters of the fabric we used numerical and physical experiments of shooting the lead bullet through the single layer of the fabric. As the lead bullet material parameters have been already determined in Section 4.2, only the fabric structure parameters remain to be qualified during this model validation step. The bullet has been shot through a large piece of the fabric ($\sim$1 m $\times$ 1 m) so the waves excited by the impact could not reach the boundaries of the fabric during the time of the perforation. The boundary conditions imposed on the model were presented as the unsupported boundaries of the fabric. Mathematically, the experimental situation can be presented as very similar to the one described in Section 2.3. The data obtained from the physical experiment were the pattern of broken yarns and maximum deflection of the fabric at the time moment of full perforation. Though at the moment we had no possibility to film the full process of the fabric perforation, the obtained results enabled to establish some key parameters of the model ensuring a satisfactory level of adequacy of the computed results against the experimental ones.

As a base assumption we used the purely elastic paraaramid material properties to the failure limit. This is a well-known experimental fact obtained by static tests of paraaramid yarns. The values of elasticity modulus E, Poisson's ratio PR and mass density RO were considered as prescribed (Table 3). The elastic failure limit of the material is modeled by assuming the plastic material with failure strain 0.04 corresponding to the yield stress $\text{SIGY} = 3.6\text{e} + 9\,\text{N/m}^2$.

The parameters values to be determined by comparing the computed results against the experimental ones are the yarn-to-yarn sliding friction coefficient FSs and bullet-to-yarn sliding friction coefficient FSk between the yarns of the woven structure and the surface of the bullet. For the sake of simplicity, we do not introduce additional parameters specifying the dependency of the friction coefficient against the velocity of sliding. It should be noticed that the established parameters are valid only for the range of velocities taking place at $\sim$300 m/s ballistic interaction.

Fig. 12 presents a sample view of the perforated fabric. The main feature directly and easily comparable with the computation results is the pattern of broken yarns. Fig. 13 presents the numeration of warps (Wp) and wefts (Wf) used in our description. The quarter symmetry model is built by using the presupposition that the bullet meets the crossing point of Wp0 and Wf0 yarns. Unfortunately, it is hardly possible to ensure such

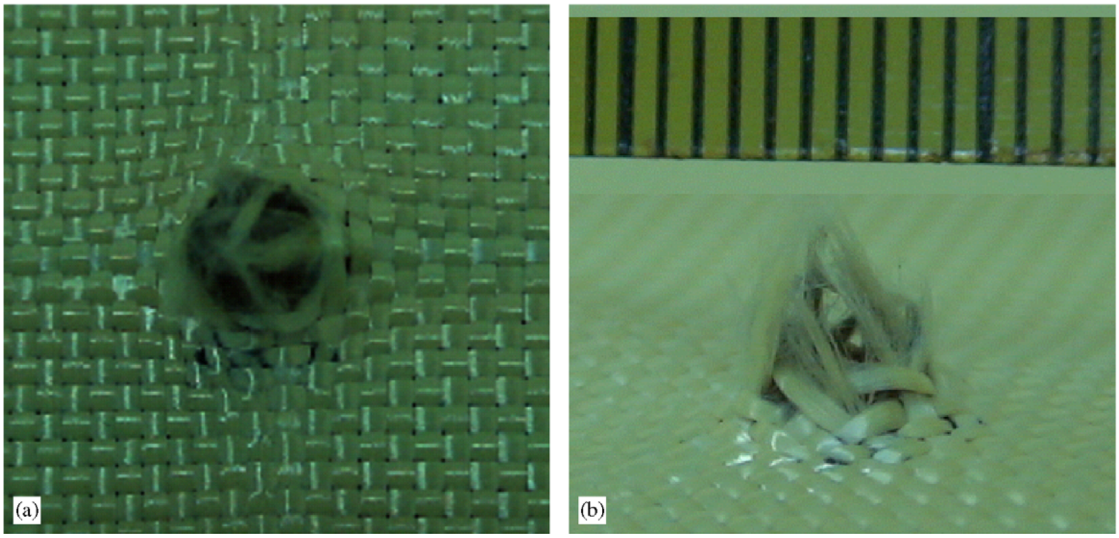

Fig. 12. Photos of a single fabric layer perforated by 6 mm lead bullet.

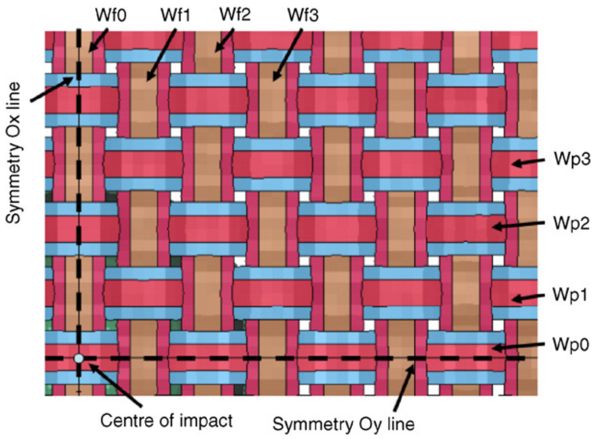

Fig. 13. Numeration of warp (**Wp**) and weft (**Wf**) yarns in the quarter-symmetry model.

accurateness of the shot, therefore generally the mathematical and experimental models may appear as not completely identical.

Fig. 14 presents some computed results obtained by using the value of friction coefficient FSs = 0.2 and three values of friction coefficient FSk = 0, 0.1, 0.2. The geometrical patterns of the yarn structure at time moments at the initiation (*ti*) and at full perforation (*tp*) the end of the fabric failure, corresponding transverse deflections of the fabric surface *zi* and *zp*, as well as, final plastic deformations (*epmax*) of the bullet are presented. Fig. 14 actually represents only characteristic sample situations. Much more computations have been performed during this investigation. The comparison of the results indicated that perforation of the fabric model by breaking four yarns (it is the most often observed case in the reality) is possible in quite narrow range of values of friction coefficients as

$$0.1 < \mathrm{FSk} < 0.2; \quad 0.1 < \mathrm{FSs} < 0.2; \quad \mathrm{FSs} + \mathrm{FSs} < 0.3.$$

Symbols Wpi and Wfi indicate the sequence of yarns broken during the ballistic interaction by using the numeration presented in Fig. 13. For example, notation Wp1, Wf1 → Wf0 → Wp0 means that at initiation of the fabric failure first warp yarn and first weft yarn are broken simultaneously, after that breaks 0th (central)

FSk	Pattern of broken yarns at the moment of initiation of the failure of the fabric	Pattern of broken yarns at the moment of full perforation	Pattern of plastic deformation zones on the tip of the bullet
0.	FSs=0.2; ti=2.4e-5; tp=2.7e-5s; zi=0.0058; zp=0.00665 **Wf0 -> Wp0 (2 broken yarns)** 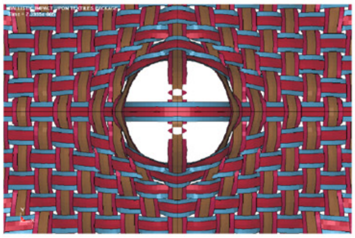	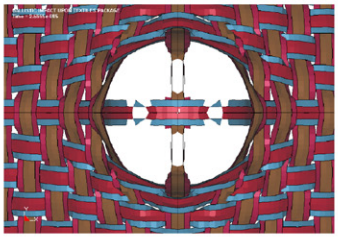	epmax=0.45 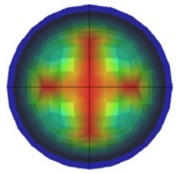
0.1	FSs=0.2; ti=2.58e-5;tp=3.36e-5s; zi=0.0063; zp=0.0082 **Wp1,Wf1 -> Wf0 -> Wp0 (4 broken yarns)** 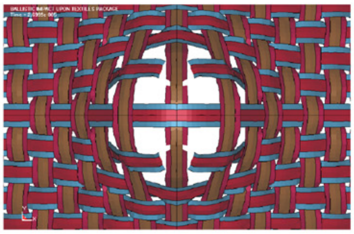	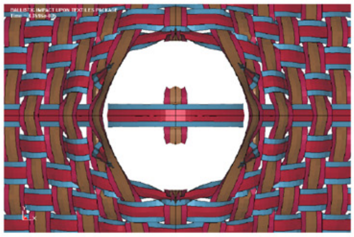	epmax=0.5 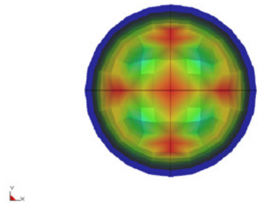
0.2	FSs=0.2; ti=3.18e-5;tp=4.68e-5s; zi=0.0077; zp=0.01166 **Wp1,Wf1 ->Wf0 ->Wp0-> ->2Wp1 (6 broken yarns)** 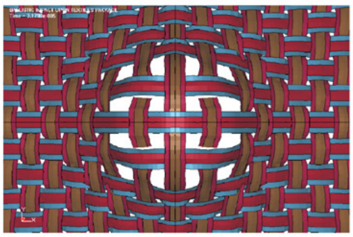 (a)	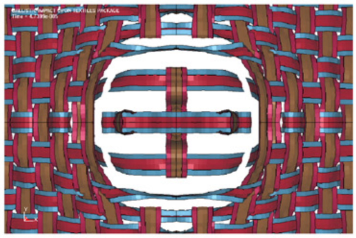 (b)	epmax=0.6 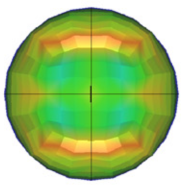 (c)

Fig. 14. Computed patterns of broken yarns at time moment of initiation of failure (a), full perforation (b) and the plastic deformation of the bullet (c) at yarn–yarn friction coefficient value FSs = 0.2 and three different values of the yarn–bullet friction coefficient FSk.

weft yarn and finally the central warp yarn. The first and second rows of figures in Fig. 14 represent the situations close to those we observed in reality, while the situation presented in the third row corresponds to larger value FSk = 0.2 and was not encountered in our experiments. The differences in-between the plastic deformation patterns of the tip of the bullet also indicate clearly expressed shift of the deformed zones to the peripheral zones of the bullet tip as the friction coefficient is increased.

The values of frictional interaction forces can be specified by employing the dynamic friction law as $F = \mathrm{FD} + (\mathrm{FS} - \mathrm{FD})e^{-\alpha|V_{\mathrm{rel}}|}$, where V_{rel}—the relative tangential velocity of contacting surfaces. Static (FS) and dynamic (FD) friction coefficients should be established by performing additional experiments. However, we use only static friction coefficient FS the value of which has been adjusted to the proper range of ballistic interaction velocities. It is unlikely to obtain very precise evaluations of the friction coefficients that could be recommended for simulations of real ballistic processes as the effective values of the coefficients may depend upon other factors, e.g., temperature and humidity. It is well known that the wet fabrics are perforated much more easily. The modeling results demonstrated that only two yarns Wp0 and Wf0 fail if the friction coefficient values are close to zero. If the bullet does not meet the crossing point of the yarns, at very small friction coefficient values the bullet goes through the fabric without breaking a single yarn.

4.4. Simulation of the impact of a bullet against a MLFP

Numerical experiments of the bullet and MLFP interaction have been performed by using the woven patch and membrane models connected by means of the tie constraint and two models of a bullet (see Section 2.1). The friction coefficient between two layers of fabric have been used the same as obtained in Section 4.3 for yarn-against-yarn sliding interaction. Very probably the values of friction coefficients between the membrane zones of the model are not of primary importance. The frictional interactions between layers at zones distant from the impact point may be considered as weak because of initial clearances between the layers of the free-fabric package, see Section 2.4. Comparisons with the physical experiment have been performed at ''integer'' level by evaluating the ability of the package to hold up the bullet. However, the results are realistic as the

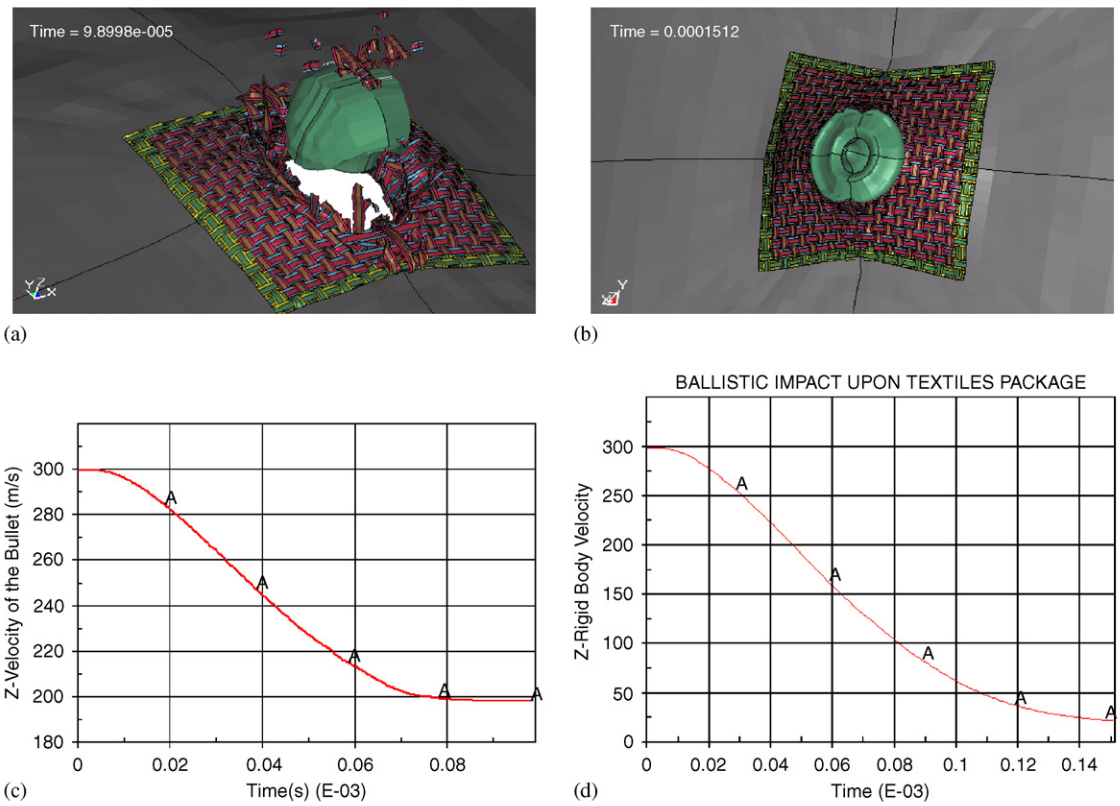

Fig. 15. A 300 m/s velocity impact of a lead bullet upon a multi-layer fabric package: (a,c) five layers of fabric, general view of the fabric package and bullet after penetration (a) and velocity time law of the bullet (c); (b,d) 12 layers of fabric, general view of the stopped bullet (b) and time law of velocity of the bullet (d).

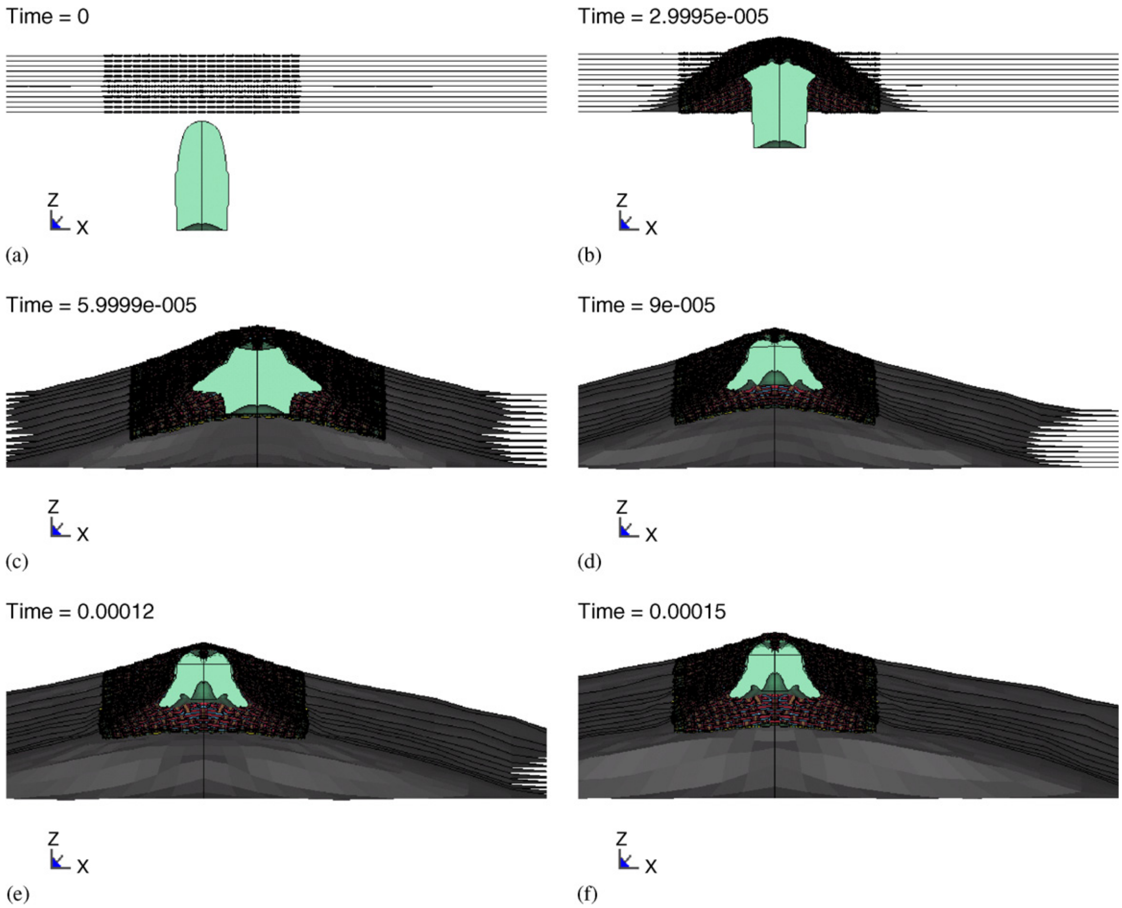

Fig. 16. Still-images (a–f) demonstrate the hold-up of the lead bullet BALLE22 (velocity 300 m/s) in the 12-layer fabric package.

overall MFLP model is constructed of the parts the dynamic behavior of which demonstrates a satisfactory coincidence with the test experiments described in Sections 4.2 and 4.3.

The obtained results indicate that 10–12 layered paraaramid MLFP package is nearly at the ballistic limit against a 6 mm lead bullet moving at 300 m/s. The bullet holdup effect decreases as the friction coefficient between layers is decreased (e.g., when the humidity of the environment increases).

Figs. 15 and 16 demonstrate the interaction process between the BALLE22 lead bullet and textile packages consisting of five fabric layers (Fig. 15a,c) and 12 layers (Fig. 15b,d) where only static material characteristics of paraaramid are employed (SRC = SRP = 0).

A series of numerical experiment results demonstrate that by employing only statically determined characteristics of materials the strength of the multi-layer textile package is obtained somewhat less than it is observed in reality. The direct and simple way to improve the adequacy of the model to reality is to assume the dependency of yield (failure) limit against the strain rate as in formula (1). The key is that the static characteristics of the material are known and the material is elastic up to its failure limit. In our model we took into account the increase the yield limit of the material due to high interaction velocity failure strain simply by increasing the failure strain to 0.046 (the static experiments indicate the value 0.04). However, more detailed analysis and the comparison of the numerical results against the results obtained from case-oriented experiments are necessary. The last Figs. 15 and 16 do not pretend to prove the full validity of the model. They rather demonstrate that the modeling results may give a good insight into the passage of the ballistic interaction and provide better understanding of the processes taking place in textile body armor.

5. Conclusions

The finite element analysis of the interaction process of paraaramid Twaron multilayer fabrics packages (MLFP) against a 6 mm bullet has been performed in LS-DYNA by taking into account real geometries and deformability of interacting parts. The main goal of the presented study was to develop a workable model suitable for simulation of the ballistic interaction of MLFP of real dimensions by employing moderate computer resources and with satisfactory level of adequacy.

The size of the model was reduced to reasonable dimensions by presenting the yarns in the woven fabrics structure as narrow bands of a prescribed cross-section and by presenting the zones of the fabric distant from the point of impact by an orthotropic membrane model. The process of shooting-through one fabric layer has been simulated and the combined model consisting of a woven patch tied to a uniform orthotropic membrane has been verified. It has been demonstrated that for obtaining models close to reality it is not sufficient to use the material properties determined by static or quasi-static experiments only. Comparisons of the computed results against the experimental ones have been performed in order to find the values of the dynamic material parameters of the model. The model has been improved by scaling the yield stress and failure strain values subject to the strain rate value.

The adjustment of model parameters in order to obtain a satisfactory match against the experiment can be regarded as a primary stage of model validation. The response of a single fabrics layer to uni-axial tension has been simulated and satisfactory coincidence of the obtained results against experimental ones has been demonstrated. Numerical and physical experiments have been performed in order to determine the dynamic material parameters of the lead bullet ensuring adequate behavior of the model. The modeling results of shooting-through one fabric layer have been compared against the experiment in terms of the pattern of broken yarns and plastic deformation of the tip of the bullet. The range of realistic values of yarn–yarn and yarn–bullet sliding friction coefficients of the model have been found.

The holdup of a bullet and the shooting-through the multilayer fabrics have been simulated. Though not fully validated, the modeling results provide a good insight into the passage of the interaction process and facilitate the comprehension of the ballistic interaction phenomena in textile structures.

The presented research suggests prospective directions of the research of the ballistic response of free-fabric structures, such as further improvement of multi-filament yarn model, ballistic interaction analysis by taking into account the biomechanical properties of human body protected by the textile packages, etc. The validation of the model is neither onetime nor fully unambiguous action. Along with improvements of the model and availability of new experimental data the perfection level of the validation is increased step by step.

Acknowledgment

The research has been sponsored by the Lithuanian Science and Studies Foundation.

References

[1] Abraitiene A, Valaseviciute L. Analysis of textile packages and ballistic characteristics o paraaramid yarns. In: Mickus KV, editor. Proceedings of the conference science and industry of Lithuania. Kaunas: Technologija; 1998. p. 242–6.

[2] Byrne C, Davies B. New yarn and fiber development drives technical textiles market. Int Fiber J 1999;2:100–2.

[3] Cunnif PM. An analysis of the system effects in woven fabrics under ballistic impact. Text Res J 1992;62(9):495–509.

[4] Tan VBC, Lim CT, Cheong CH. Perforation of high strength fabric by projectiles of different geometry. Int J Impact Eng 1992;28(2):207–22.

[5] Shim VPW, Tan VBC, Tay TE. Modeling deformation and damage characteristics of woven fabric under small projectile impact. Int J Impact Eng 1995;16(4):585–605.

[6] Duan Y, Keefe M, Bogetti TA, Cheeseman BA. Modeling the role of friction during ballistic impact of a high strength plain-wave fabric. Compos Struct 2005;68(3):331–7.

[7] Clegg R, et al. Application of a coupled anisotropic material model to high velocity impact response of composite textile armor. In: 18th international symposium and exhibition on ballistics, San Antonio, Texas, USA, November 15–19, 1999, Century Dynamics, Inc. TP052.

[8] Barauskas R, Vilkauskas A. Modeling of bullet interaction against the life protection textile. In: Proceedings of the Nordic LS-DYNA users' conference, Gothenburg, Sweden, 2002, Engineering Research Nordic AB (Proceedings on CDROM).

[9] Tarafaoui M, Akesbi S. A finite element model of mechanical properties of plain weave. Colloids Surf A: Physicochemical Eng Aspects 2001;187–188:439–48.
[10] Boisse P, Gasser A, Hivet G. Analyses of fabric tensile behavior: determination of the biaxial tension-strain surfaces and their use in forming simulations. Compos Part A 2001;32:1395–414.
[11] LS-DYNA theoretical manual. Livermore Software Technology Corporation, May 1998.
[12] Barauskas R, Abraitiene A. Modelling of a Bullet Interaction Against the Multilayer Textile Package in LSDYNA. In: Tsahalis DT, editor. Proceedings of the first international conference from scientific computing to computational engineering, Athens, Greece, 2004 (Proceedings on CDROM).